UDC 551.509.313:551.513.1

GLOBAL REAL-DATA FORECASTS WITH THE NCAR TWO-LAYER GENERAL CIRCULATION MODEL

DAVID P. BAUMHEFNER

National Center for Atmospheric Research,* Boulder, Colo.

ABSTRACT

A number of global real-data numerical forecasts have been calculated using the two-layer NCAR (National Center for Atmospheric Research) general circulation model. The purpose of these experiments was threefold: 1) to evaluate the model's ability to predict the real atmosphere, 2) to develop a global forecasting model which will make use of the data obtained by the proposed GARP (Global Atmospheric Research Program), and 3) to help determine some of the internal, empirical constants of the model. In order to evaluate the accuracy of the predictions, several "skill scores" were calculated from the forecasted and observed variables. A by-product of this research was the testing of five different types of data-initialization schemes. Over 50, 4-day forecasts have been run, in which the initialization schemes and internal constants were varied.

The results from these experiments indicate that the present two-layer model is capable of forecasting the real atmosphere with reasonable skill out to 2 days at the surface and 4 days in the middle troposphere. The best initialization scheme for this particular model, thus far, appears to be the complete balance equation. However, several of the simplified initialization techniques are very close in terms of forecasting skill.

1. INTRODUCTION

Considerable progress has been made during the past few years in the field of real-data numerical weather prediction. Perhaps the most important contribution has been the formulation of several elaborate primitive equation models such as those of Shuman and Hovermale (1968) and Miyakoda and Smagorinsky (1969). However, both of these models dealt with only the Northern Hemisphere. The current literature contains only one report on global primitive equation forecasting (Miyakoda and Staff Members 1968) in which the authors discuss the results of a 2-week global forecast using a nine-level model. The lack of research on the problem of global real-data forecasting can be attributed in part to the absence of readily obtainable conventional data in the Tropics and Southern Hemisphere. This barrier is rapidly being overcome by the use of high-speed communication networks and by objective interpretation of satellite information over data-sparse regions.

The global study to be discussed in this paper used data that were extracted from the 1958 IGY observation period. These data were found adequate for defining the large-scale features of the global circulation. The global real-data forecasting project was started at The National Center for Atmospheric Research (NCAR) with three basic purposes in mind: 1) to evaluate the model's ability to predict the real atmosphere and compare the results with other numerical models, 2) to develop a global forecasting model to check the usefulness of the data obtained by the proposed GARP worldwide data network; and 3) to help determine some of the internal empirical constants of the model. As a by-product of research along these guidelines, five different initialization schemes were tested and several verification parameters were evaluated. This paper will concentrate mainly on a comparison of the various initialization techniques and a discussion of a 4-day forecast with the two-layer model.

Since January 1967, over 50 cases have been run. Each case has included a 4-day forecast and computation of several verification statistics, requiring approximately 100 min per case on the Control Data Corporation 6600.

2. DESCRIPTION OF THE FORECAST MODEL

The basic forecast equations used in the real-data forecast experiments are shown below (Kasahara and Washington 1967).

Momentum equations:

$$\frac{\partial}{\partial t}\rho u=-\nabla\cdot\rho u\mathbf{V}-\frac{\partial}{\partial z}\rho uw-\frac{1}{a\cos\phi}\frac{\partial p}{\partial\lambda}+\left(f+\frac{u}{a}\tan\phi\right)\rho v+\mathbf{F}_\lambda. \quad (1)$$

$$\frac{\partial}{\partial t}\rho v=-\nabla\cdot\rho v\mathbf{V}-\frac{\partial}{\partial z}\rho vw-\frac{1}{a}\frac{\partial p}{\partial\phi}-\left(f+\frac{u}{a}\tan\phi\right)\rho u+\mathbf{F}_\phi. \quad (2)$$

Pressure tendency equation:

$$\frac{\partial p}{\partial t}=g\rho w-g\int_z^{z_t}\nabla\cdot\rho\mathbf{V}dz+B;\qquad B=\frac{\partial p}{\partial t}\Big|_{z_T} \quad (3)$$

where z_T denotes the top of the model atmosphere. $\mathbf{F}_\lambda$ and $\mathbf{F}_\phi$ are frictional terms.

Richardson equation:

$$w=-\int_0^z\nabla\cdot\mathbf{V}dz-\frac{1}{\gamma}\int_0^z\frac{1}{p}(B+J)dz+\frac{1}{c_p}\int_0^z\frac{Q}{T}dz \quad (4a)$$

* The National Center for Atmospheric Research is sponsored by the National Science Foundation.

where $J=\mathbf{V}\cdot\nabla p-g\int_z^{z_T}\nabla\cdot\rho\mathbf{V}dz$ and Q denotes the net heating or cooling rate.

Pressure tendency $(\partial p/\partial t)$ at $z=z_T$:

$$\left.\frac{\partial p}{\partial t}\right|_{z_T}=\frac{\frac{1}{\gamma}\int_0^{z_T}\frac{J}{p}dz-\frac{1}{c_p}\int_0^{z_T}\frac{Q}{T}dz+\int_0^{z_T}\nabla\cdot\mathbf{V}dz}{-\frac{1}{\gamma}\int_0^{z_T}\frac{dz}{p}}. \quad (4b)$$

The momentum and pressure tendency equations specify the time change of the horizontal velocity and pressure, while the Richardson equation determines the vertical velocity diagnostically at each time step.

The model formulation considered in this paper is a basic two-layer design (fig. 1) in which the pressure is defined at the surface and at 6-km and 12-km levels and the horizontal velocity is prescribed at the 3-km and 9-km levels. The vertical velocity is computed at 6 km. The horizontal mesh is 5° latitude by 5° longitude and extends over the entire globe. The model is capable of determining the effects of friction, sensible and latent heat, and long- and short-wave radiation. A more detailed description of these processes is found in Kasahara and Washington (1967). For the boundary-layer exchanges with the free atmosphere, the average January distribution of the surface temperature is used in place of a surface temperature calculation.

The model used in these experiments is an earlier version of the present more complete model in which the dynamic effects of orography, the surface temperature calculation, and the prediction of water vapor field are now included. The more complete model including the details of numerical calculations and the finite-difference schemes are described in Washington and Kasahara (1970).

3. DATA ACQUISITION

The period of Jan. 15–19, 1958, was selected for the first series of forecast experiments. Two meteorological variables (pressure and velocity) were analyzed semi-independently for this study. The pressure analyses (1200 GMT only) were obtained from several different sources. Height analyses for 1000, 500, and 200 mb in the Northern Hemisphere were acquired from the National Meteorological Center. For the Tropics, surface and 500 mb, data were obtained from the German Weather Service analysis of the IGY period and the 200-mb geopotential was analyzed from original microcard data by the author. For the Southern Hemisphere, data at the surface and 500 mb were extracted from the South African Weather Bureau published analyses, and the 200-mb height data were provided by H. van Loon of NCAR. The geopotential values at 500 and 200 mb were hydrostatically converted to pressure at the 6-km and 12-km levels and manually interpolated to 5° × 5° Intersections.

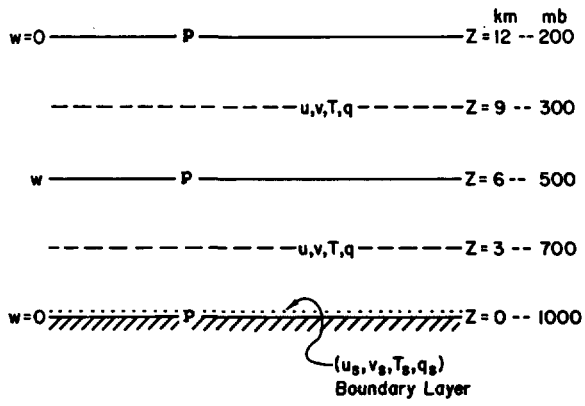

FIGURE 1.—Vertical structure of the two-layer model without orography. T is temperature, p is pressure, u and v are the wind components, and q is specific humidity.

The observed horizontal velocity data were processed in a unique manner. First, the vertical distribution of the wind from the individual soundings was punched on cards for the 5-day period. Then, in order to provide more complete coverage, some of the off-time reports were averaged together to produce data at 1200 GMT. After the time-averaging process, each sounding was vertically averaged from the surface to 6 km and from 6 km to 12 km. This procedure, which corresponds to the vertical structure of the two-layer model, eliminates most small-scale noise in the original wind data. Each averaged wind was then plotted, and streamline and isotach fields were constructed from the data. The final step was to determine the direction and speed at each grid point from the analyses.

The ultimate form of the data used by the model included grid-point values of pressure at three levels and velocity at two levels. Only the Jan. 15, 1958, 1200 GMT data were used as the initial state for the forecast; data for the other days were used for verification. The data have been processed in a form that is easily reproducible on magnetic tape or punched cards.

4. VERIFICATION TECHNIQUES

Some criteria of success or failure are needed in real-data forecasting to guide the researcher toward the best possible method. In this paper, the measure of success is based entirely on several "skill scores," or verification parameters, which are derived from differences between the observed and forecasted states of the atmosphere. Although this choice may be somewhat arbitrary, these objective scores appear to be adequate for the present study.

The four scores used to compare forecasts with observed conditions are: the root mean square of the pressure difference (RMS–P); the S_1–P score of the pressure (Teweles and Wobus 1954); the root mean square of the magnitude of the wind vector difference (RMS–V); and the root mean square of the wind speeds difference (RMS–

SP). The definitions of these scores are as follows:

$$\text{RMS–A}=\left[\frac{\sum(A_x^o-A_x^F)^2\cos\phi}{\sum\cos\phi}\right]^{1/2} \quad (5)$$

where A is any scalar quantity and

$$\text{S}_1\text{–P}=100\frac{\sum|(P_x^F-P_{x+1}^F)-(P_x^o-P_{x+1}^o)|}{\sum|(P_x-P_{x+1})^{o\text{ or }F}|}. \quad (6)$$

The superscript indicates whether the quantity is observed or forecasted, and the subscript refers to grid-point location. The summations may be taken over a limited area (for example, North America) or over the entire globe. After comparing the behavior of the individual scores with the actual maps of the observed minus forecasted values, the RMS–P score was found to be a good measure of the absolute value of the pressure field, while the S_1–P score was much more sensitive to the gradient and position of pressure configurations. The RMS–V score was shown to be a good indicator of the magnitude and direction of the observed and forecasted wind maxima, and the RMS–SP score proved to be a good check of the absolute magnitude of the velocity.

The correlation coefficient of the observed pressure change compared to the forecasted pressure change was also calculated. After extensive comparisons with other scores and visual interpretation, the correlation coefficient was found to be quite erratic in nature. For example, in some cases, the score was actually better at the end of 4 days than at the end of the first 24-hr period (figs. 6 through 9). This may have been due to the particular case selected, in which most of the major storms did not translate but remained stationary and intensified. From our experiences, at least, the correlation coefficient which was calculated from our forecasts was a poor indicator of the skill contained in a real-data forecast.

The methods selected for judging the skill of the forecasts were put to one further test. Several different smoothers were applied to the forecasted pressure before the verification calculation was made. The five-point smoother

$$\overline{A}_{I,J}=(4A_{I,J}+A_{I+1,J}+A_{I-1,J}+A_{I,J+1}+A_{I,J-1})/8 \quad (7)$$

where I and J denote grid coordinates, the nine-point smoother

$$\overline{A}_{I,J}=[\alpha A_{I,J}+\beta(A_{I+1,J}+A_{I-1,J}+A_{I,J+1}+A_{I,J-1}) +A_{I+1,J+1}+A_{I-1,J+1}+A_{I-1,J-1}+A_{I+1,J-1}]/16 \quad (8)$$

where $\alpha=4.0$ and $\beta=2.0$, and the nine-point smoother-amplifier (Stackpole 1968) where the first pass is made with $\alpha=4.0$ and $\beta=-2.0$ and the second pass with $\alpha=36.0$ and $\beta=-6.0$ were calculated. The results of these experiments are shown in figure 2. All the smoothing techniques tested improved the forecast verification except for the RMS–P at 6 km, where the stronger smoothers acted to increase the measured error. After examining the original unsmoothed forecast pressures, it was found that the 6-km values were much smoother than the surface pressures, which offers a partial explanation for the different behavior of the RMS–P in the vertical. By using a smoothing technique on the forecasted variables, an increase in apparent forecast skill of approximately 10–20 percent was realized. It is not clear from figure 2 which type of smoothing should be used, but from visual examination the nine-point smoother amplifier contained the most detail in the smoothed fields. Therefore, in all subsequent experiments, this technique was chosen for all verification calculations.

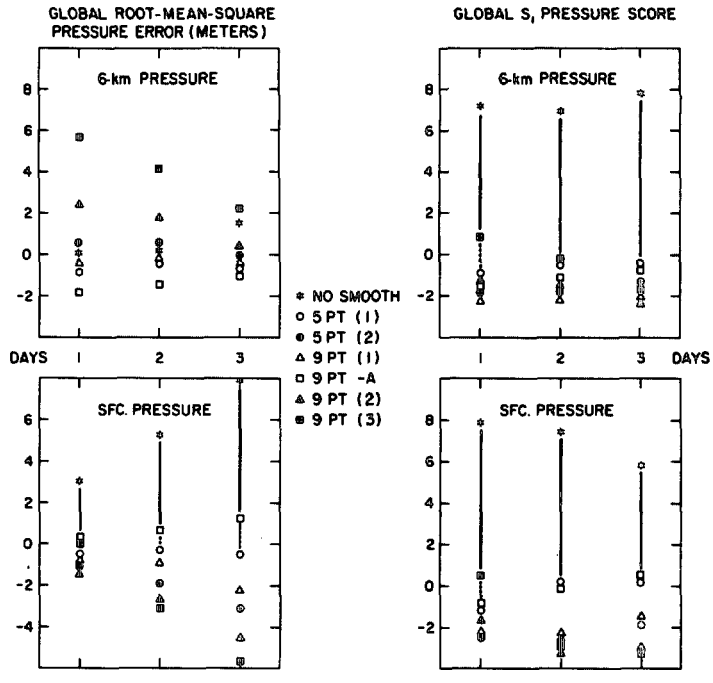

FIGURE 2.—Smoothing comparison case 57. Comparison of different types of smoothers and their effect on the verification score. The ordinate is a score value that was subtracted from the mean of all cases for each day. The list in the center of the figure indicates the different kinds of smoothers tested. The figures within parentheses after each identification show how many times each smoother was passed through the field. The 9 PT–A stands for the smoother-amplifier procedure.

5. INITIALIZATION

Because the primitive equation models are capable of calculating gravity waves as well as meteorologically significant waves, it is usually advisable to suppress the gravity wave mode from the initial data. This process, known as initialization, can be performed in several different ways. The pressure or mass field may be held fixed, and the velocity field is then calculated or "balanced." Inversely, the velocity field may be held fixed, and the pressure field calculated. Another possible initialization scheme, which is not discussed in this paper, makes use of the forecast equations to filter out the un-

wanted wave mode (for example, Miyakoda and Moyer 1968).

There appears to be some disagreement in the literature (Ellsaesser 1968) as to which method of initialization is the best for forecasting with real data. In order to investigate this problem, it was decided to test five different variations of initialization on a global scale. The theory leading to these initialization techniques is discussed by Houghton and Washington (1969). The five methods are written in spherical coordinates:

1) complete balance equation (B)

$$\nabla^2\psi=\frac{1}{\rho f}\nabla^2P-\frac{\beta}{fa^2}\frac{\partial\psi}{\partial\phi}-\frac{2}{fa^2}J\left(\frac{1}{\cos\phi}\frac{\partial\psi}{\partial\lambda},\frac{\partial\psi}{\partial\phi}\right)+\frac{1}{fa^4}\left(1+\tan\phi\frac{\partial}{\partial\phi}\right)\left[\left(\frac{\partial\psi}{\partial\phi}\right)^2+\left(\frac{1}{\cos\phi}\frac{\partial\psi}{\partial\lambda}\right)^2\right], \quad (9)$$

2) geostrophic balance equation (BG+J)

$$\nabla^2\psi=\frac{1}{\rho f}\nabla^2P-\frac{\beta}{f^2\rho a^2}\frac{\partial P}{\partial\phi}+\frac{2}{f\rho a^2}J\left(\frac{1}{f\cos\phi}\frac{\partial P}{\partial\lambda},\frac{1}{f}\frac{\partial P}{\partial\phi}\right)+\frac{1}{f^2\rho^2a^4}\left(1+\tan\phi\frac{\partial}{\partial\phi}\right)\left[\left(\frac{\partial P}{\partial\phi}\right)^2+\left(\frac{1}{\cos\phi}\frac{\partial P}{\partial\lambda}\right)^2\right], \quad (10)$$

3) linear balance equation (BG−J)

$$\nabla^2\psi=\frac{1}{f\rho}\nabla^2P-\frac{\beta}{f^2\rho a^2}\frac{\partial P}{\partial\phi}, \quad (11)$$

4) mixed velocity-pressure equations (BV) where the observed pressure is held fixed

$$\nabla^2\psi=\frac{1}{f\rho}\nabla^2P-\frac{\beta}{f^2\rho a^2}\frac{\partial P}{\partial\phi} \quad (12)$$

and where the observed velocity is held fixed

$$\nabla^2\psi_K=\mathbf{k}\cdot\nabla\times\mathbf{V}_{obs} \quad (13)$$

and

$$\nabla^2P=\rho f\nabla^2\psi_K+\frac{2\rho}{a^2}J\left(\frac{1}{\cos\phi}\frac{\partial\psi_K}{\partial\lambda},\frac{\partial\psi_K}{\partial\phi}\right)+\frac{\rho\beta}{a^2}\frac{\partial\psi_K}{\partial\phi}=\frac{\rho}{a^4}\left(1+\tan\phi\frac{\partial}{\partial\phi}\right)\times\left[\left(\frac{\partial\psi_K}{\partial\phi}\right)^2+\left(\frac{1}{\cos\phi}\frac{\partial\psi_K}{\partial\lambda}\right)^2\right], \quad (14)$$

5) geostrophic equations (G)

$$u=\frac{1}{2}\left(-\frac{fa}{\tan\phi}+\sqrt{\frac{a^2f^2}{\tan^2\phi}-\frac{4}{\rho\tan\phi}\frac{\partial P}{\partial\phi}}\right) \quad (15)$$

and

$$v=\frac{\partial P}{\partial\lambda}\Big/\left[\left(f+\frac{u}{a}\tan\phi\right)a\rho\cos\phi\right]. \quad (16)$$

In equation (9), method (B), the observed pressure may be altered to satisfy the elliptic condition (Houghton and Washington 1969). Equation (10), method (BG+J), avoids the elliptic condition by inserting the geostrophic wind in place of the stream function in all the terms on the right-hand side of (9). Equation (11), method (BG−J), is a linearized version of (BG+J) in which the Jacobian and spherical terms have been dropped. The fourth method (BV) is a hybrid form which uses the linearized balanced equation (12) in polar and midlatitudes, and solves the kinematic (wind field) stream function (13) and then the pressure balance equation (14) in the Tropics. The latitude changeover between observed pressure and observed wind may be varied from Pole to Equator. However, for the first comparison test, it was set at 40° N. and S. Equations (15, 16), method (G), represent the geostrophic velocity, which is used for the initial condition along with the observed pressure.

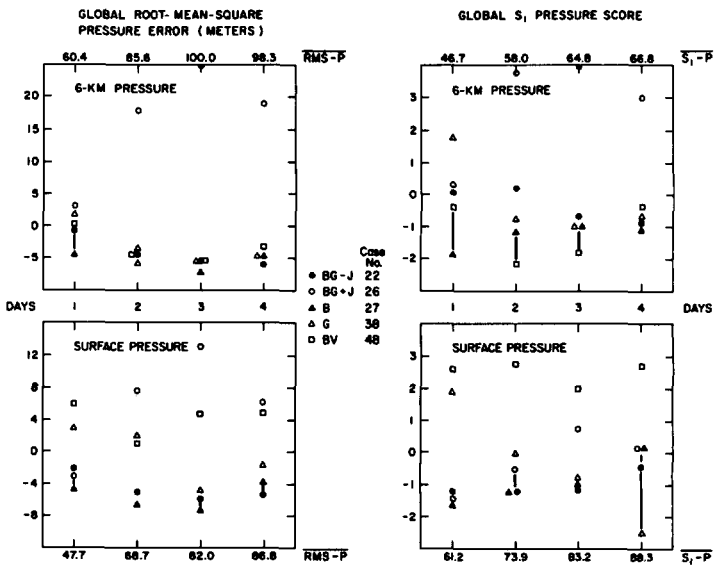

FIGURE 3.—Comparison of five initialization schemes with the RMS-P and S_1-P skill scores. The values on the ordinate are normalized from the average score, which is printed at the top or bottom of each square for each day. The center legend refers to the various initialization techniques as described in the text.

The comparison between the various initialization schemes was made by forecasting with each method out to 4 days, holding the internal functions of the model constant. Neither diabatic effects nor initial divergence was included in the forecasts. It was anticipated that the verification scores would then indicate which initialization equation produced the best forecast. The results of the comparisons are illustrated in figures 3 and 4.

The most surprising result of this experiment was the relatively small differences among the various methods when compared to the total error of the forecast. Only one initialization scheme, method (BG+J), was clearly inferior to the others. Although it is somewhat difficult to determine the "best" method from the figures, it appears that method (B) holds a slight edge in the pressure verification scores (fig. 3), while the mixed pressure-velocity initialization (BV) shows its superiority in the velocity scores (fig. 4). It is interesting to note from this experiment that the linearized form of the balance equation (BG−J) approaches the same accuracy as the solution of the complete balance equation (B).

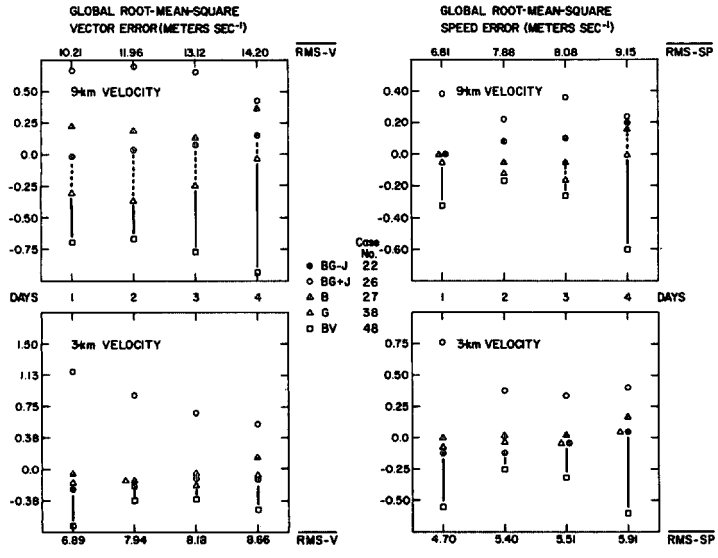

FIGURE 4.—Same as figure 3, with the RMS–V and RMS–SP scores at 3 and 9 km for velocity fields.

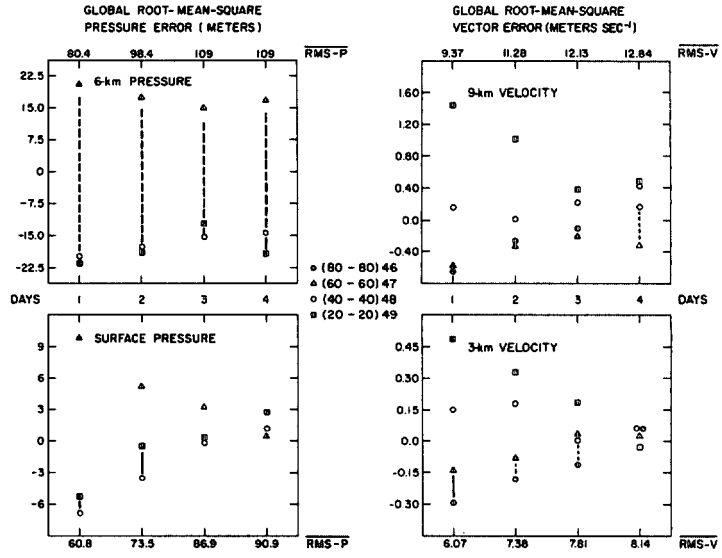

FIGURE 5.—Comparison of forecasts in which the latitude changeover from the observed pressure to the observed velocity was varied in the mixed velocity-pressure initialization scheme. The ordinate is the normalized value of the particular verification score as printed at the top or bottom of the square. The latitudes at which changeover occurred are indicated within parentheses in the center legend.

The relatively poor surface pressure scores of method (BV) can be partially explained in the following way. Since in the two-layer model the horizontal wind velocity is carried at the intermediate levels (3 and 9 km), the inversion of the balance equation from the kinematic stream function gives the pressure at the wrong level. A linear interpolation-extrapolation scheme is used to solve for the pressure at the surface and at 6 and 12 km. In order to accomplish the calculation, a third variable must be assumed, namely the lapse rate. The extrapolation of the pressure from 3 km to the surface is, therefore, somewhat inaccurate and probably accounts for the poor scores. It seems likely that a six-layer version of the model will show an improvement in the pressure extrapolation technique.

Some further experimentation was conducted with the mixed velocity-pressure initialization scheme. A series of forecasts were made with an adiabatic model in which the latitude of the changeover between pressure and wind was varied from 20° N. and S. to 80° N. and S. The results are plotted in figure 5. The verification scores do not distinguish any particular position of the latitude changeover as best; the pressure scores show a preference for the lower latitude values, while the velocity scores indicate the opposite. The relaxation technique, used to solve the initialization methods, seems to be playing a part in the behavior of the verification scores. When the latitude changeover is a low value, 20° N. and S., the wind field is being derived through a relaxation scheme which results in a smoother pattern than the observed velocity. The situation works the opposite way when the latitude changeover has a high value. It appears from these preliminary results that a compromise value, 40° N. and S., may be used to some advantage. More experimentation with the scheme to improve the handling of the derived variable is underway.

As an extension of the initialization research, one other possibility was investigated; the observed pressure and the observed velocity were used as the initial condition without any attempt at balancing the two fields. The model produced a 4-day forecast without numerical instability destroying the forecast. However, after a 24- to 36-hr period, in which the gravity wave mode tended to lower the accuracy of the forecast, the verification scores for 6 km were slightly better than those of the initialized forecasts. This is a somewhat surprising result, since one might expect that initializing the observed variables should yield a better forecast. Further research on this problem is being planned.

6. A 4-DAY FORECAST

The forecast with the best skill to date, as indicated by the verification scores, is examined in detail in this section. The initialization of the real data was accomplished with the complete balance equation, method (B). The divergent part of the wind was not calculated for the initial state. All diabatic effects were included except for the saturated form of the latent heat parameterization. The initial pressure fields along with the appropriate verification and forecast maps are shown in figures 6 to 9. Several verification scores for certain regions of the globe are also displayed next to the forecasted fields in order to judge more easily the skill of the predicted maps.

The 24-hr forecast of the sea-level pressure (fig. 6) exhibits a fair amount of skill when compared to the

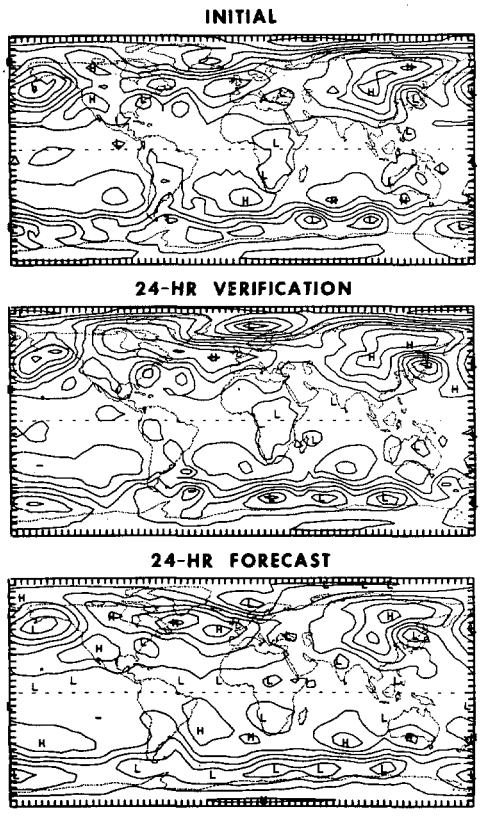

FIGURE 6.—The 24-hr forecast of sea-level surface pressure shown with the initial state and verification patterns on a cylindrical map projection with equal latitude-longitude intersections. The RMS–P and S_1–P skill scores are referred to in the text except CC, which is the correlation coefficient of the pressure change of the initial and forecasted values. The velocity scores refer to the 3-km level and are in m sec^{-1}. The isobars are drawn every 8 mb.

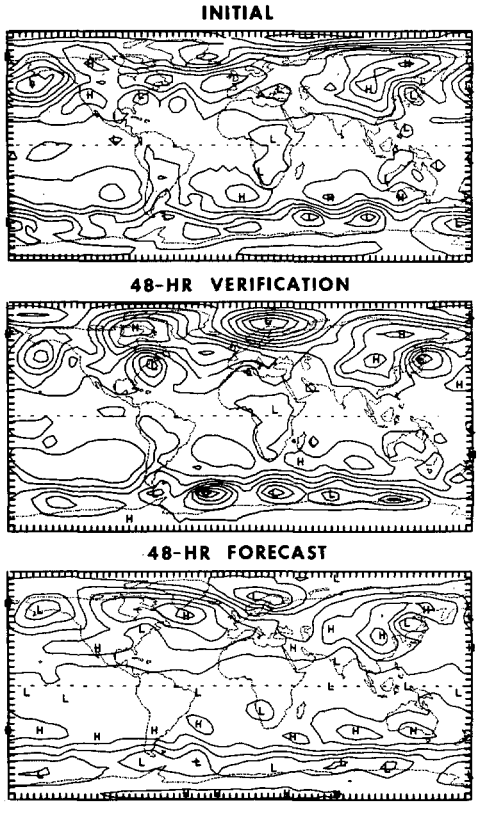

FIGURE 7.—Same as figure 6, for 48-hr forecast of the surface pressure.

verification pattern. The developing Low just off the coast of Greenland is correctly predicted to move rapidly eastward and intensify. The two systems adjacent to the American and Asian coasts are properly forecasted to remain near the coastline; however, the intensity of all three storms was underforecasted by 10 to 20 mb. The strength and position of the high-pressure systems are forecasted fairly well except for a 27-mb error southeast of Greenland, where a secondary Low developed on the verification chart. The translation of the midlatitude storms in the Southern Hemisphere is forecasted quite well, but again the intensity of the system is underestimated. The root mean square of the pressure indicates an average error of 4.4 mb over the globe, while the S_1–P score shows approximately the same skill at 24 hr that the NMC (National Meteorological Center) surface forecasts, made with a six-layer model, have at 30 hr (Shuman and Hovermale 1968).

By the time the forecast has reached 48 hr (fig. 7), the skill shown by the surface pressure prediction was minimal. The central pressure of the three major storms in the Northern Hemisphere is in error by over 30 mb. The most obvious defect of the forecast is the gradual weakening of the surface pressure gradients over the entire globe. This problem was also present in hemispheric forecasts derived from a more complicated model used by Miyakoda et al. (1969). Although the root mean square of the pressure is only 6.3 mb at 48 hr, which is still below the value obtained from a persistence forecast, the S_1–P score indicates very little skill in the prediction. On the other hand, after examining the forecast carefully, a few areas of success can be seen. The development of the Norwegian Sea storm is forecasted quite well, except for the intensity, and the predicted positions of all major Lows over the globe are fairly good.

In the 6-km forecast at 48 hr (fig. 8), there appears to be more skill associated with this level than with the surface pressure forecast at the same time. The development of the Norwegian Sea storm is quite accurately predicted. The phase of the two Northern Hemisphere coastal storms is slightly behind that shown on the verification map, but the amplitude of both waves is forecast fairly well. The synoptic scale prediction in the Southern Hemisphere does not enjoy the same measure of skill as in the Northern Hemisphere. Most of the disturbances have been severely truncated. The skill scores also indicate this trend, with the highest value of the S_1–P score appearing in the global category. Overall, the RMS–P scores are higher and the S_1–P scores are lower for the

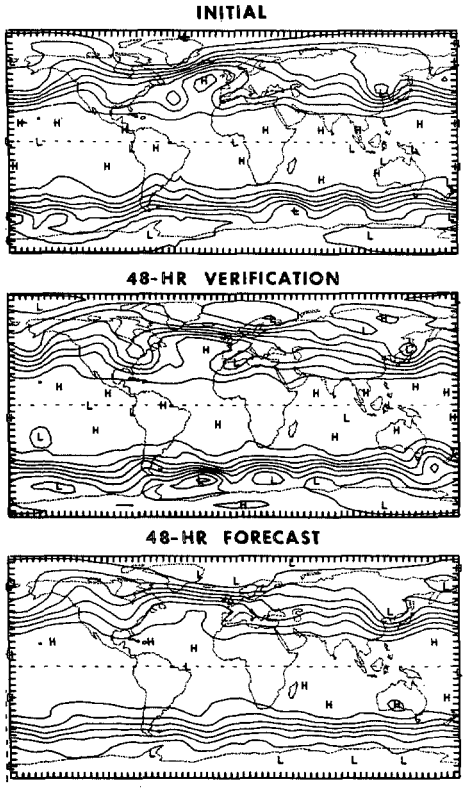

FIGURE 8.—Same as figure 6, for 48-hr forecast of the 6-km pressure The velocity scores refer to the 9-km level.

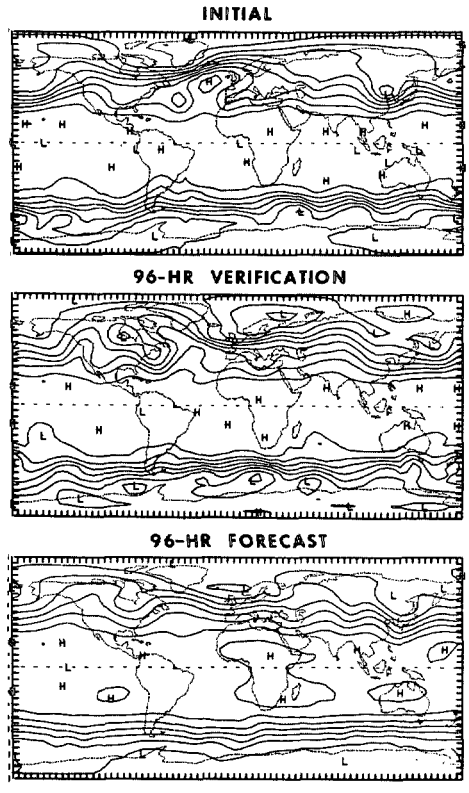

FIGURE 9.—Same as figure 6, for 96-hr forecast of the 6-km pressure.

6-km forecast than the surface-pressure verification values.

At 96 hr (fig. 9), the forecast accuracy of the synoptic scale has deteriorated beyond any usefulness. The global verification scores also show the deterioration, with an average pressure error of nearly 8 mb and the S_1–P score approaching a zero skill value. It is interesting to note that, as in the case of the surface pressure, the root mean square of the 6-km pressure (RMS–P) has not reached the value of a persistence forecast at 96 hr. This is probably due to the major intensifications of the North American and Norwegian Sea systems. The forecasts of the longer wavelengths (for example, wave number 4), however, do exhibit some skill at the end of 4 days. For example, the long-wave ridge just west of Europe has retrograded westward nearly 25° of longitude and the high-latitude trough has moved to the east, in agreement with the verification map. In the Southern Hemisphere, the amplitude of the longer waves was quite small at the initial time; hence, after 4 days, all that is left is zonal flow.

After examination of all the maps and verification scores, the overall usefulness of this global real-data forecast is judged to be about 48 hr for the surface pressure and 96 hr for the 6-km pressure.

7. ADDITIONAL EXPERIMENTS

In order to determine the effects of the various diabatic terms in the equations on the real-data forecasts, three experiments were run in which 1) all diabatic effects were included, 2) the latent heat term was removed, and 3) all diabatic effects were removed. Figure 10 illustrates the RMS–P for the three cases. It is evident from the verification scores that the inclusion of the latent heating term in the equations is detrimental to the skill of the real-data forecast. The apparent failure of the latent heat term can be traced to the basic assumption made in the early version of the general circulation model that the atmosphere is completely saturated. This assumption leads to a continual pumping of heat into the atmosphere, raising the mean temperature, which is reflected by the RMS score. This phenomenon was not observed in the S_1–P score, which uses only the gradient of pressure. In fact, the case including all the diabatic terms showed a slightly better S_1–P score than the rest. Therefore, one may conclude that the saturated form of the latent heat release is a poor approximation for real-data numerical prediction. The other diabatic effects, such as sensible heat and radiation, appear to improve the forecast with time, but their contribution to the total skill of the forecast is quite small up to 4 days.

Some preliminary attempts were made to calculate the divergent part of the velocity field for the initial condition of the forecast. To date, three separate formulations have been tested, and three forecasts have been produced with the new initial states. The results indicate that the addition of an initial divergence has a small overall effect on the forecasts. A slight improvement is noticed in regions of strong cyclogenesis, where the vertical motion

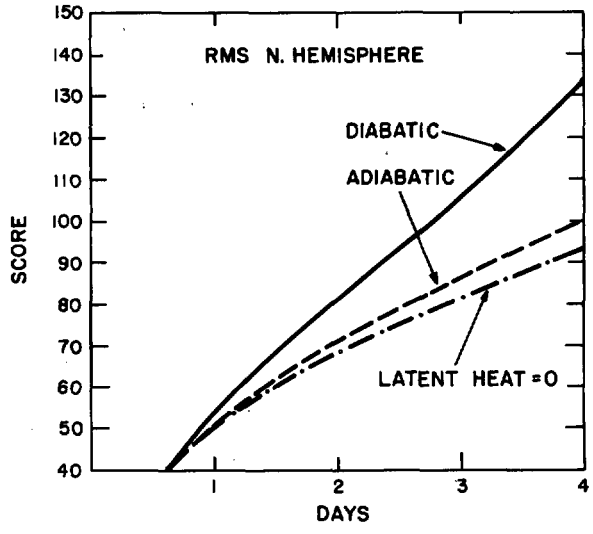

FIGURE 10.—Root mean square of the pressure (RMS–P) for several forecasts that tested various diabatic effects of the model. The ordinate values are in meters.

is most intense. The main reason for the apparent insensitivity of the model to the divergent initial condition may be related to the large mesh size (5°×5°), which controls the magnitude of the synoptic scale vertical motion. The typical vertical velocity value in the real-data forecasts is about 1–2 cm sec^{-1}, which obviously does not affect the horizontal motions to any great extent in just 4 days.

A six-layer general circulation model, which has reduced the vertical mesh by a factor of 2, is currently being tested with real data. Preliminary forecasts from this model have provided a comparison of the mesh reduction when contrasted with the two-layer real-data forecasts. Both the two-layer and the six-layer model now have the capability of taking the actual terrain into account. The method of including the terrain has been briefly described by Kasahara and Washington (1968). Several experiments are under way in which the effect of orography on real-data predictions is being examined. Also, a complete hydrological cycle has been added to the model, and this will allow further experimentation with the diabatic effects and their relationship to real-data forecasts.

8. CONCLUSIONS

A number of global real-data forecasts have been successfully produced by the two-layer NCAR general circulation model. Several specific conclusions have been drawn from these experiments and are summarized below.

1) The best initialization scheme for this particular model, thus far, appears to be the complete balance equation. However, several of the simpler versions are very close in terms of forecasting skill. After further experimentation, the mixed velocity-pressure method may prove to be superior to other schemes.

2) The correlation coefficient of the pressure change is a poor measure of the skill of our real-data forecasts when compared to other verification scores.

3) A saturated form of the latent heat parameterization appears to be a poor assumption for our real-data forecasts.

4) The inclusion of a divergent component in the initial state has little effect on the outcome of the forecast.

5) The experimental predictions seem to indicate that a a 5°×5° latitude-longitude mesh is too coarse to resolve the synoptic scale disturbances accurately.

6) The forecasting usefulness of the two-layer model is judged from these experiments to be approximately 48 hr for the surface pressure and 96 hr for the 6-km or mid-tropospheric pressure.

ACKNOWLEDGMENTS

The real-data forecast research program has been a joint effort by Drs. A. Kasahara, W. Washington, D. Houghton, and the author. I would like to thank N. Paris of the NCAR Publications Department for the careful editing done on the manuscript. Appreciation is also expressed to A. Kasahara, W. Washington, J. Fankhauser, and D. Williamson for their reviews of the paper.

REFERENCES

Ellsaesser, Hugh W., "Comparative Test of Wind Laws for Numerical Weather Prediction," *Monthly Weather Review*, Vol. 96, No. 5, May **1968**, pp. 277–285.

Houghton, David, and Washington, Warren, "On Global Initialization of the Primitive Equations: Part I," *Journal of Applied Meteorology*, Vol. 8, No. 5, Oct. **1969**, pp. 726–737.

Kasahara, Akira, and Washington, Warren M., "NCAR Global General Circulation Model of the Atmosphere," *Monthly Weather Review*, Vol. 95, No. 7, July **1967**, pp. 389–402.

Kasahara, Akira, and Washington, Warren M., "Thermal and Dynamical Effects of Orography on the General Circulation of the Atmosphere," paper presented at the WMO/IUGG Symposium on Numerical Weather Prediction, Tokyo, Nov. 26–Dec. 6, **1968**.

Miyakoda, K., and Moyer, R. W., "A Method of Initialization for Dynamical Weather Forecasting," *Tellus*, Vol. 20, No. 1, Feb. **1968**, pp. 115–128.

Miyakoda, K., and Staff Members, "Extended Prediction With a Nine-Level Model on the Kurihara Grid," paper presented at the WMO/IUGG Symposium on Numerical Weather Prediction, Tokyo, Nov. 26–Dec. 6, **1968**.

Miyakoda, K., Smagorinsky, J., Strickler, R. F., and Hembree, G. D., "Experimental Extended Predictions With a Nine-Level Hemispheric Model," *Monthly Weather Review*, Vol. 97, No. 1, Jan. **1969**, pp. 1–76.

Shuman, Frederick G., and Hovermale, John B., "An Operational Six-Layer Primitive Equation Model," *Journal of Applied Meteorology*, Vol. 7, No. 4, Aug. **1968**, pp. 525–547.

Stackpole, John D., "Smoothing in the 6-Layer (PE) Numerical Prediction Model," *Technical Procedures Bulletin* No. 10, Weather Analysis and Prediction Division, ESSA, Weather Bureau, Feb. 8, **1968**, 8 pp.

Teweles, Sidney, Jr., and Wobus, Hermann B., "Verification of Prognostic Charts," *Bulletin of the American Meteorological Society*, Vol. 35, No. 10, Dec. **1954**, pp. 455–463.

Washington, Warren M., and Kasahara, Akira, "A January Simulation Experiment With the Two-Layer Version of the NCAR Global Circulation Model," *Monthly Weather Review*, Vol. 98. **1970**, (to be published).

[Received August 14, 1969; revised October 6, 1969]